Interface diffusion kinetics and lifetime scaling in multilayer Bragg optics

R. W. E. van de Kruijs*[a], S. Bruijn[a], A. Yakshin[a], I. Nedelcu[a], F. Bijkerk[a,b]
[a]FOM Institute for Plasma Physics Rijnhuizen, Edisonbaan 14, Nieuwegein, the Netherlands;
[b]MESA+ Institute for Nanotechnology, University of Twente, Enschede, the Netherlands

ABSTRACT

The internal structure of Mo/Si multilayers is investigated during and after thermal annealing. Multilayer period compaction is shown to result from diffusion induced $MoSi_2$ interlayer growth, reducing optical contrast and changing the reflected wavelength. We focus on early-stage interface growth observed at relatively low temperatures (100 °C - 300 °C), determining diffusion constants from parabolic interface growth laws. Diffusion constants obey Arrhenius-type behavior, enabling temperature scaling laws. Using the methods developed, we compare results on Mo/Si based multilayers designed for enhanced thermal stability and discuss their relevant diffusion behavior. Arrhenius-type behavior can be observed in all multilayers studied here, and demonstrates reduction of diffusion rates over several orders of magnitude. The method described here is of general interest for any multilayer application that is subjected to enhanced thermal loads and demonstrates the enormous technology gain that this type of optics has experienced the last decade.

Keywords: Multilayers, EUV lithography, optical coatings, diffusion, interfaces, x-ray diffraction

1. INTRODUCTION

Multilayer reflective coatings play an enabling role in the development of optics for the VUV to x-ray wavelength range, with applications ranging from microscopes and solar telescopes to x-ray free electron lasers and EUV photolithography[1-4]. In general, such applications all demand stable optics performance over extended periods of time in environments that are potentially harmful to the optics or are difficult to access for optics maintenance. The technological challenge to develop stable multilayer coatings for such applications can only be addressed by an improved understanding of the basic multilayer structure and its response to environmental factors.

Due to the high optical contrast in the EUV wavelength range, Mo/Si based multilayers are good candidates for reflective coatings that are designed for use above the Si L-edge (wavelength above 12.5 nm). Near the edge, Mo/Si multilayer coatings are able to reflect up to 70% of the radiation that is incident normal to the multilayer surface. The multilayer typically consists of several tens of layer pairs of approximately equal thickness Mo and Si layers, with exact layer stack design depending on application wavelength (extinction depth) and geometry. The internal structure generally consists of polycrystalline Mo layers and amorphous Si layers, separated by the naturally formed sub-nm thick silicide interfaces. Changes to this internal structure due to radiation and/or thermal loading result in a reduced optical performance and should therefore be avoided.

In this study, we address the changes to the Mo/Si multilayer structure when exposed to thermal annealing. We focus on the initial period and reflectivity changes during annealing that occur at relatively low temperatures, with the aim of developing scaling laws relevant for applications. We address the process of interlayer formation that is responsible for optics degradation and discuss methods to reduce interlayer formation in order to develop thermally stable multilayers, demonstrating diffusion constants that are reduced by several orders of magnitude.

*kruijs@rijnhuizen.nl; phone 31 306096854; fax 31 306031204

Advances in X-Ray/EUV Optics and Components VI, edited by Christian Morawe, Ali M. Khounsary, Shunji Goto,
Proc. of SPIE Vol. 8139, 81390A · © 2011 SPIE · CCC code: 0277-786X/11/$18
doi: 10.1117/12.893546

Downloaded From: https://www.spiedigitallibrary.org/conference-proceedings-of-spie on 2/28/2018 Terms of Use: https://www.spiedigitallibrary.org/terms-of-use

2. EXPERIMENTEL SETUP

The multilayer samples discussed in the work have been prepared using a deposition facility consisting of a UHV chamber (base pressure 10^{-9} mbar) equipped with electron beam evaporation and DC magnetron sputtering. Working pressure during magnetron sputtering was 10^{-4} mbar. Additional ion bombardment can be applied for surface smoothening, film densification, or ion implantation. Typical deposition rates for electron beam evaporated and magnetron sputtered samples are between 0.01 nm/s and 0.1 nm/s. Layer thickness control for magnetron sputtered samples is achieved by calibrated deposition rates, while for electron beam evaporation, calibrated quartz mass balances were used. The multilayer period was chosen to be 7 nm for all samples, to obtain maximum reflectivity around 13.5 nm. Further sample details are discussed in the next sections.

The deposition facility is connected through a transfer stage where samples can be transported (under 10^{-10} mbar) to an X-ray Photoemission Spectroscopy (XPS) chamber with additional SEM and AES capability. XPS depth profiles can be performed using low energy (500 eV in this study) ion sputtering, as well as through non-destructive angle resolved XPS measurements.

Hard x-ray analysis is performed using a Panalytical X'Pert diffractometer (Cu-$K_{\alpha 1}$, E = 8.0 keV, λ = 0.15406 nm). Grazing incidence measurements (GIXR) were carried out ex-situ after deposition and after annealing cycles as well as in-situ during annealing studies. Wide angle x-ray diffraction (XRD) measurements are performed in a modified Bragg-Brentano geometry to maximize diffracting volume, while the samples were rotated 20 degree in-plane to suppress diffraction from substrate lattice planes.

Soft-X-ray reflectivity measurements at 1.5 degree off-normal incidence angle with respect to the sample plane were taken in the 13 nm - 14 nm wavelength range at the SX700 beamline of PTB at the BESSY2 synchrotron in Berlin[5].

3. MULTILAYER STRUCTURE DURING ANNEALING

3.1 Diffusion in Mo/Si multilayers

The structure of Mo/Si based multilayers is known to degrade when exposed to high temperatures[6]. As an example, Figure 1 shows a transmission electron micrograph image of the internal structure of a Mo/Si multilayer, before and after being exposed to thermal treatment. In this example, a 30 minute exposure to 400 °C was sufficient to completely change the internal structure of the multilayer. The layered structure has strongly compacted, changing the reflected wavelength for a fixed angle of incidence. The optical contrast is also reduced, and interfaces appear more ragged, reducing the multilayer reflectance. In addition, the crystalline structure of the layers has also gone through large changes.

The kind of damage shown in Figure 1b is actually far beyond what can be tolerated in most practical applications based on Mo/Si multilayer coated optics. To study the damage in more detail, grazing incidence X-ray reflectometry (GIXR) measurements have been carried out as a function of annealing temperature, using a vacuum chamber with base pressure 10^{-7} mbar. Annealing times of 48 hours were chosen to allow near-saturation of the thermal damage. Samples were annealed sequentially in the temperature range from T = 75 - 375 °C, increasing temperatures by steps of 25 °C, with post-annealing GIXR measurements after each temperature step. Separate experiments confirmed that direct annealing to a specific temperature yielded the same results as sequentially annealing. From the GIXR measurements, the multilayer period can be readily determined by fitting the positions of the Bragg diffraction peaks to the modified Bragg's law

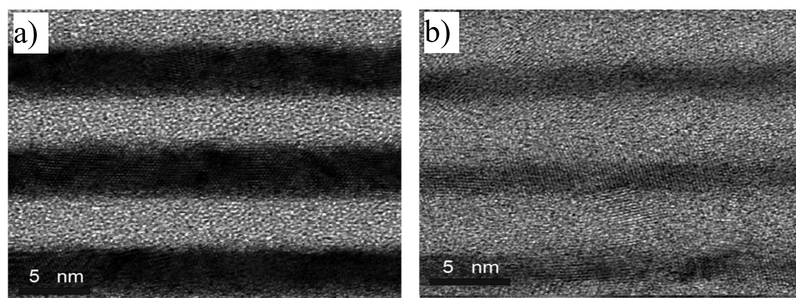

Figure 1. Transition Electron Microscopy images of a multilayer cross-section before (a) and after (b) exposure to a high thermal load. Thermal damage consists of reduced optical contrast and reduced multilayer period.

Downloaded From: https://www.spiedigitallibrary.org/conference-proceedings-of-spie on 2/28/2018 Terms of Use: https://www.spiedigitallibrary.org/terms-of-use

given by[7] $m\lambda = 2d\sin\theta\sqrt{1-\frac{2\delta}{\sin^2\theta}}$, where m represents the Bragg order, λ and θ are the wavelength and grazing angle of incidence of the x-ray beam, and d and δ are the multilayer period and average value of (1-n) with n the real part of the refractive index, respectively.

Figure 2 shows the change in the multilayer period obtained from GIXR measurements, as a function of temperature for different values of $\Gamma = d_{Mo}/(d_{Mo}+d_{Si})$ in the multilayer. A Mo-to-Si ratio of $\Gamma = 0.4$ is often used for obtaining highest reflectivity at a wavelength of 13.5 nm, while lower or higher values may be relevant for e.g. stress-compensation layers or reflective coatings in other wavelength ranges. In general, the data shows a continuous decrease of the multilayer period with increasing temperature, up to 300 °C. When considering the temperature range T > 300 °C, it appears that the multilayer structure has gone through a transition, where the period "saturates", and this stage corresponds to the structure observed after annealing in the TEM measurements discussed above. The final level of period reduction is actually determined by the initial Mo-to-Si ratio, and is connected to the formation of molybdenum-silicides from the available amounts of Mo and Si, i.e. for low and high values of Γ, only a limited amount of silicide can form before running out of Mo or Si, while for Γ = 0.4, almost all available Mo and Si can react to form a silicide.

For the temperature range T < 300 °C, it appears that the change in the multilayer period is nearly the same for 0.4 < Γ < 0.7. This observation immediately suggests that the thermal damage observed here cannot be linked to changes in the bulk Mo and Si layers, but must be attributed to changes at the interfaces. In literature, thermally induced growth of molybdenum silicide interfaces is indeed generally accepted as the mechanism that leads to reduction of the multilayer period. It should be noted here that for Γ < 0.4, and for Γ > 0.7, the thermal damage actually does depend on Γ, as the structure of the as-deposited multilayer is fundamentally different (i.e. different Mo crystallinity, different initial interface formation, reduced availability of materials for interface formation, etc.). Finally, no differences in thermal damage were observed when comparing multilayers produced using electron beam evaporation and DC magnetron sputtering, suggesting that minor differences in the as-deposited multilayer structure such as stress level, layer crystallinity, and bulk densities do not significantly influence the processes of interface formation that are responsible for the period change.

Figure 1 shows that thermal exposure not only leads to a reduced multilayer period, but also leads to reduced optical contrast between the layers. For this reason, a change in the multilayer period due to thermal loading is in general accompanied by a reduction in the multilayer peak reflectivity. To investigate the relation between period and reflectivity changes, for Γ = 0.4, experiments were carried out for various annealing times (1-100 hrs) and various temperatures in the range from T = 50 – 200 °C, and resulting reflectivity losses and period changes are plotted in Figure 3. This figure

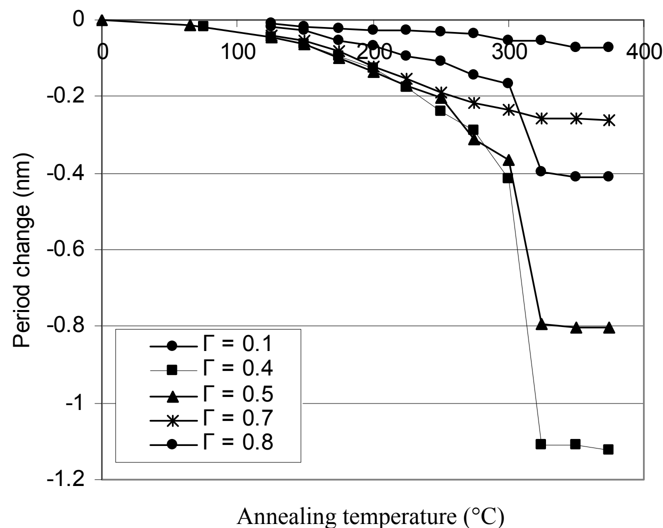

Figure 2. Change in multilayer period as a function of annealing temperature for sequential 48hr annealing cycles. Data is shown on multilayer with various Γ (Mo-to-Si) ratios in the multilayer.

Downloaded From: https://www.spiedigitallibrary.org/conference-proceedings-of-spie on 2/28/2018 Terms of Use: https://www.spiedigitallibrary.org/terms-of-use

suggests that there exists a relation between the period change and the observed reflectivity losses, as indicated by the dashed line.

Assuming that the period change is solely due to growth of silicide interface layers, it should be possible to calculate the reflectivity loss that would result from such interface growth. The solid lines in Figure 3 represent reflectivity calculations performed using IMD[8]. The upper curve represents calculations based on a model that assumes $MoSi_2$ interface growth, while the lower curve is based on a model that assumes Mo_3Si interface growth. For the reflectivity calculations, bulk layer and interface densities were assumed, and the initial interface thicknesses in the model were taken as 0.5 nm on top of Mo and 1 nm on top of Si, based on TEM investigations[9]. It should be noted that there remains an uncertainty in the actual layer densities and stoichiometries of the growing interfaces, although allowing for variations in densities by up to 10 %, the calculated reflectivity values did not change significantly.

The increasing discrepancy between experimental data and model simulations reported in Figure 3 was attributed to enhanced surface oxidation at enhanced temperatures, resulting in additional reflectivity losses. Furthermore, the differences between the various model simulations are relatively small, suggesting that, although the experimental data can be of use for predicting reflectivity losses, it can not be used to obtain additional information about the details of interface formation. Finally, it should be noted that for most applications it is actually the reflectance loss at a fixed incidence angle and/or wavelength that is important. This reflectivity loss strongly depends on the spectral/angular shape of the reflectance peak, and is generally much larger than the change in maximum peak reflectivity shown in Figure 3.

A more detailed study on the process of thermally induced interface formation in Mo/Si multilayers has been reported in ref [9], where a combination of GIXR, XRD, and TEM experiments were carried out in the temperature range from T = 100 - 300 °C for a Mo/Si multilayer with $\Gamma = 0.4$. From the ratios of the decrease in Mo layer thickness (XRD, TEM), decrease in Si layer thickness (TEM), decrease in period (GIXR), and growth of interfaces (TEM), it was concluded that only formation of $MoSi_2$ at the interfaces can explain the experimental data. Formation of $MoSi_2$ is also energetically favorable, and XRD indeed shows the appearance of $MoSi_2$ crystallites upon annealing at T >> 300 °C, extending in depth over several multilayer periods when further annealed up to T = 800 °C. It should be noted that the crystalline state of the multilayer at 800 °C depends on the Γ ratio, and is determined by the maximum possible energy release upon formation of silicides, i.e. for high deposited Mo amounts it becomes favorable to form high Mo containing compounds such as Mo_3Si and Mo_5Si_3[10].

Assuming that the period compaction observed in Figure 2 can be fully attributed to $MoSi_2$ interface formation, it is now possible to calculate the amount of interface formed during the annealing experiments. For $MoSi_2$, using bulk densities of $\rho_{Mo} = 10.2$ g/cm^3, $\rho_{Si} = 2.32$ g/cm^3, and $\rho_{MoSi2} = 6.3$ g/cm^3, it is calculated that for each 0.1 nm of period reduction during annealing, an additional 0.25 nm of $MoSi_2$ will be formed at the interfaces[9]. Assuming diffusion limited interface growth, we can calculate an effective interdiffusion constant D^* from the annealing time and calculated interface

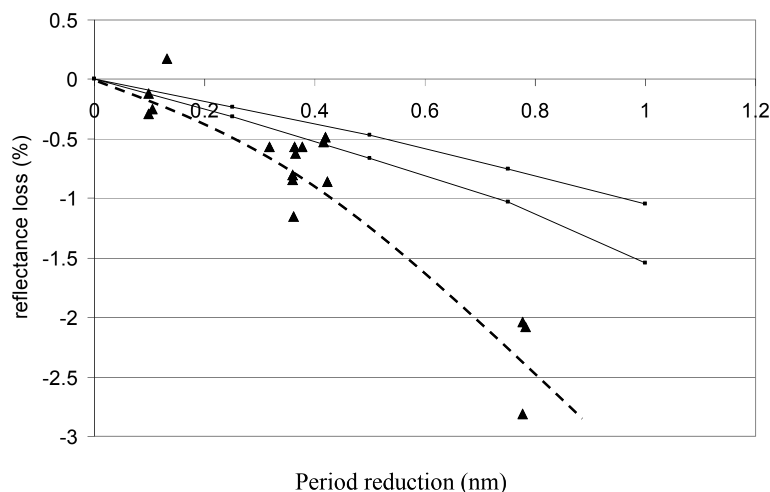

Figure 3. Reflectance loss as a function of the period reduction for a 50×[Mo/Si] multilayer with Γ=0.4, annealed at various temperatures and times. The dashed line is a guide to the eye, solid lines are based on model simulations as described in the text.

Downloaded From: https://www.spiedigitallibrary.org/conference-proceedings-of-spie on 2/28/2018 Terms of Use: https://www.spiedigitallibrary.org/terms-of-use

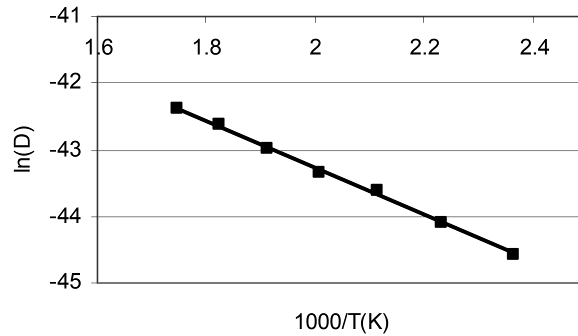

Figure 4. Plot of ln D* as a function of 1000/T, for a 50×[Mo/Si] multilayer with Γ=0.4, annealed sequentially (48hr cycles) from T = 100 °C and T = 275 °C.

thicknesses[11]. Resulting values of ln(D*) are plotted in Figure 4 as a function of 1/T.

The data plotted in Figure 4 suggests that diffusion induced interface growth in Mo/Si multilayers shows typical Arrhenius-type behavior given by $D^* = D_0 \exp(-E_A / kT)$, with E_A the activation energy, k the Bolzmann constant, and D_0 the pre-exponential factor. This result suggests the data can be used to predict diffusion induced changes in the multilayer period for a specific application temperature. In reality, interpreting these data using Arrhenius plots proves difficult, since this method ignores possible contributions from initial stage reaction limited interface growth, as well as possible changes in interface stoichiometry during interface growth. As a result, the apparent activation energy obtained from these data is lower than typical values reported in literature.

To investigate the changes in the multilayer at the very early stage of interface growth, where the period change is in the order of 0.1 nm or even lower, hard x-ray reflectivity measurements were carried out in-situ during annealing[12]. Data collection and treatment were optimized to enable determination of changes in the multilayer period with an accuracy better than 1 pm, a detection limit well below that available from diffusion studies using e.g. TEM-analysis or tracer methods. Figure 5 shows the period change as a function of annealing time for a Mo/Si multilayer with Γ = 0.4, for various annealing temperatures in the range [100 °C – 275 °C]. The data reveals a fast initial reduction of the multilayer period, which already takes place during the ramp-up of the multilayer temperature, occurring typically within several minutes. After this initial reduction, the multilayer period continues to reduce slowly over time.

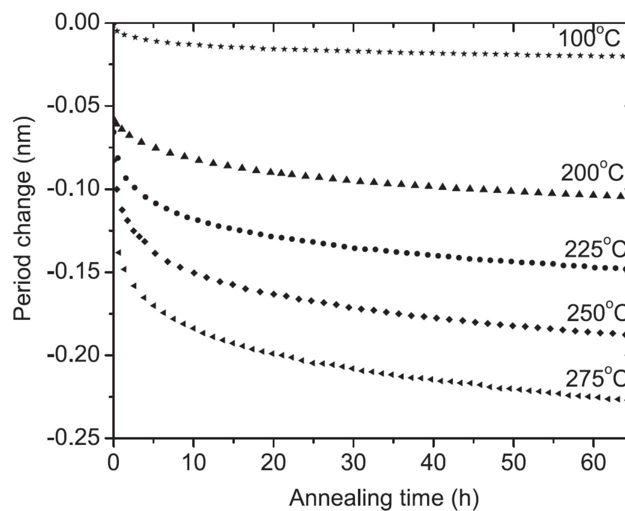

Figure 5. Period change as a function of annealing time for a 50×[Mo/Si] multilayer with Γ=0.4, annealed between T = 100 °C and T = 275 °C.

Downloaded From: https://www.spiedigitallibrary.org/conference-proceedings-of-spie on 2/28/2018 Terms of Use: https://www.spiedigitallibrary.org/terms-of-use

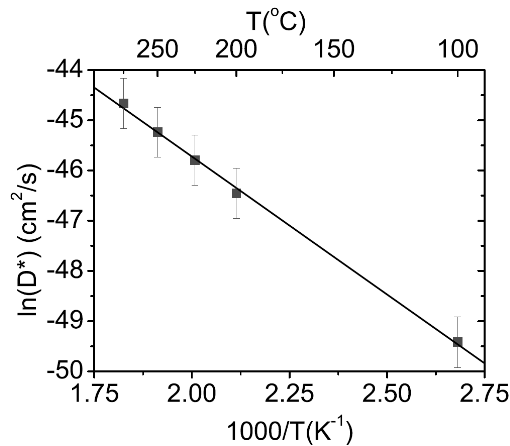

Figure 6. ln(D) as a function of 1000/T for a 50×[Mo/Si] multilayer with Γ=0.4, annealed between T = 100 °C and T = 275 °C.

We attribute the fast initial decrease of the ML period to rapid changes at the interface, possibly due to reaction limited interface growth from neighboring Mo and Si atoms, or rearrangement of existing silicides. The slow changes in the multilayer period that follow can be attributed to interface growth that is diffusion limited, and behaves according to the parabolic interface growth law[12]. From these data, diffusion constants can be determined and Figure 6 shows an Arrhenius plot obtained for the temperature range T = 100 - 275 °C. It should be noted that the activation energy is still below that reported in literature, which might be attributed to the dominance of grain boundary diffusion at low temperatures, although a changing activation energy due to changing interface composition with increasing interface thickness cannot be ruled out.

3.2 Multilayers with enhanced thermal stability

Understanding of the diffusion mechanisms responsible for silicide formation at the interfaces is only the first step in improving thermal resistance. The next step aims to eliminate or at least sufficiently reduce the speed of silicide formation. A more thermally stable multilayer can be designed by placing additional thin layers between Mo and Si that act as diffusion barriers, reducing the speed of $MoSi_2$ formation. Such materials should aim to satisfy many requirements general to thin film diffusion barriers as given in ref.[13], but in addition should not compromise the EUV reflectivity of the multilayer. Suggested diffusion barriers include silicides, carbides, borides, and nitrides. Although the thermal stability has been demonstrated to improve upon use of such barriers, it is not always easy to determine what the exact materials interactions are that govern the diffusion behavior at the Mo-to-Si interfaces.

To demonstrate the different thermal behavior that may occur in Mo/Si multilayers with increased thermal stability, as an example Figure 7 shows multilayer period changes as a function of annealing time for Mo/Si, $Mo/Si/Si_3N_4$, $Mo/B_4C/Si/B_4C$, and Mo_2C/Si multilayers. All multilayers were designed for high reflectance, i.e. Γ was experimentally optimized to obtain maximum reflectance. The data shown in Figure 7 were obtained at 250 °C, but additional experiments were carried out in the range from 100 °C to 600 °C. Compared to standard Mo/Si multilayers, all other multilayer designs shown here exhibit enhanced thermal stability. First, consider multilayers with Si_3N_4 diffusion barriers. The Si_3N_4 barrier was applied solely on the Mo-on-Si interface, since this interface has a much higher $MoSi_2$ formation rate compared to the Si-on-Mo interface[15]. In addition, the impact of barrier layers on the EUV reflectivity is lowest when such barriers are applied at the Mo-on-Si interfaces, due to the relatively low EUV absorption in the barrier layer connected with a node in the electric field at these interfaces. In this design, barrier thickness was chosen such as to match the EUV reflectivity with that of a multilayer without barriers (69 % at normal incidence at 13.5 nm). The formation enthalpy of Si_3N_4 is much lower than that of $MoSi_2$, and the barrier can be expected to be stable upon annealing. XPS analysis confirmed this expectation. From Figure 7 it is clear that the multilayer with Si_3N_4 barriers indeed exhibits improved thermal stability upon annealing, although $MoSi_2$ formation still take places with a reduced formation rate due to the reduced diffusion speed through the Si_3N_4 barrier layer.

Downloaded From: https://www.spiedigitallibrary.org/conference-proceedings-of-spie on 2/28/2018 Terms of Use: https://www.spiedigitallibrary.org/terms-of-use

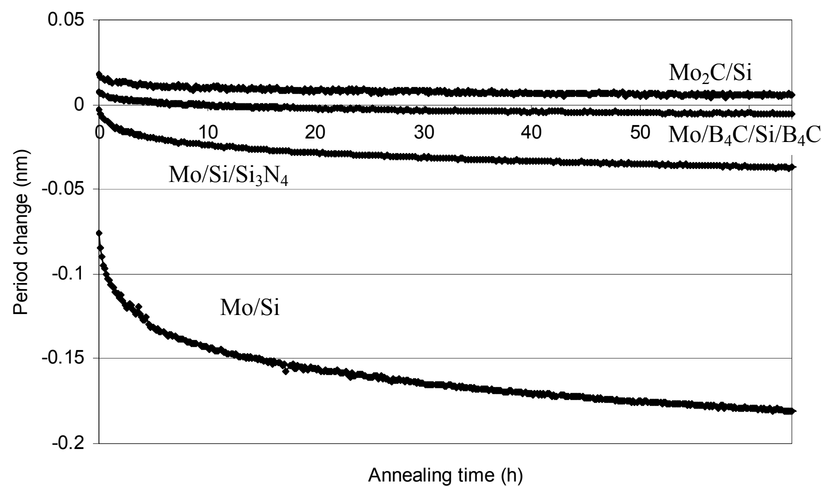

Figure 7. Multilayer period change as a function of annealing time at T = 250°C for 50×[Mo/Si], 50×[Mo/Si/Si_3N_4], 50×[Mo/B_4C/Si/B_4C] and 50×[Mo_2C/Si] multilayers.

Another barrier layer material that is often considered due to its favorable optical constants is B_4C. As an example, Figure 7 also shows multilayer period data taken on Mo/B_4C/Si/B_4C multilayers during annealing at 250 °C. In this case, barrier layers are present at all Mo-Si interfaces and required barrier layer thicknesses will depend on the expected thermal load and application-driven demands for required thermal stability. In this particular design, the enhanced thermal stability that is observed with respect to the Mo/Si/Si_3N_4 multilayer effectively comes at the cost of peak EUV reflectivity which was reduced from 69 % to 67 %. Due to the much higher formation enthalpy compared to Si_3N_4, there is no guarantee that the B_4C barrier is stable with respect to annealing. In effect, already during deposition of the B_4C barriers there appears a strong interaction with the Mo and Si layers, where Mo and Si based carbides and borides are formed[14]. In this way, the barrier layer does not act as a physical barrier that slows down interdiffusion, but instead forms a new chemical composition that effectively passivates the interfaces to Mo and Si. The complex interplay between different compounds being formed during annealing can be recognized in Figure 7 as an initial expansion of the multilayer structure, followed by further compaction and is currently the topic of further investigation. It should be noted here that the barrier quality is critical in determining the diffusion behavior. A 10 % increase in B_4C barrier layer density has been shown to reduce diffusion rates by over one order of magnitude.[16]

Diffusion barriers may strongly reduce diffusion rates across interfaces, but can never fully eliminate $MoSi_2$ formation since the latter process remains energetically favorable as long as pure Mo and Si remain present. Another method to reduce interface formation actually aims at removing the diffusing Mo and Si species by using stable compounds of Mo and Si as base materials for the multilayer. It is preferred that compound materials are used that have formation enthalpies below that of $MoSi_2$ formation, such that the system is already in its energetically most favorable state upon deposition. The drawback of this method is the relatively large impact on EUV reflectance, since the basic high optical contrast between Mo and Si has now been replaced by a reduced contrast between Mo-based and Si-based compound layers. As an example, Figure 7 shows period changes during annealing for Mo_2C/Si based multilayers. The thermal stability of this design is similar to that of the design using B_4C barriers and exhibits a peak reflectivity of 64 %. It should be noted here that the formation enthalpies for $MoSi_2$ and SiC are comparable and slightly below that of Mo_2C, suggesting that the small changes observed in the multilayer period could be due to decomposition of Mo_2C in favor of formation of either SiC or $MoSi_2$. It should be noted that the observed period changes for Mo_2C/Si and Mo/B_4C/Si/B_4C at 250 °C are below 0.01 nm, which hinders further detailed investigations into the thermal damage mechanisms for these systems. Higher temperature studies could provide information on compound formation upon annealing, although there is no certainty that exactly the same diffusion processes occur at lower temperatures.

To investigate the temperature scaling of the thermal damage to the multilayers, diffusion constants were determined from the data in the range [100 – 600 °C], and plotted in Figure 8. All multilayers show scaling of diffusion constants that is consistent with Arrhenius-like behavior. It should be noted here that the diffusion constants plotted in Figure 8 are obtained assuming only $MoSi_2$ interface growth resulting from the measured period reductions. In reality, the process of

Downloaded From: https://www.spiedigitallibrary.org/conference-proceedings-of-spie on 2/28/2018 Terms of Use: https://www.spiedigitallibrary.org/terms-of-use

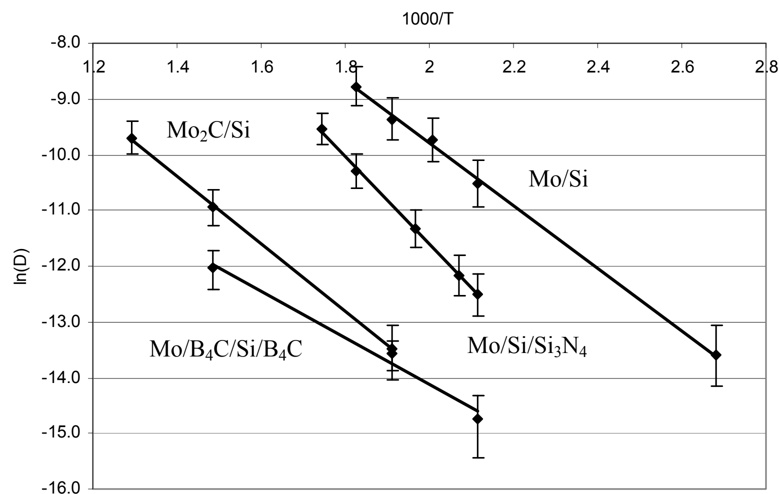

Figure 8. Arrhenius type plot comparing diffusion constants in 50×[Mo/Si], 50×[Mo/Si/Si_3N_4], 50×[Mo/B_4C/Si/B_4C] and 50×[Mo_2C/Si] multilayers.

period change may result not only from $MoSi_2$ formation, but also from compounds formed by Mo and/or Si reacting with the barrier layer materials. It is therefore disputable whether the values of E_A obtained using this method represent actual activation energies for a single diffusion process, or represent an effective process of interface formation. However, Figure 8 does demonstrate that diffusion rates in Mo/Si based multilayers can be suppressed over several orders of magnitude, empirically scaling with temperature according to Arrhenius-like behavior and showing potential for being used in improving and predicting optics thermal lifetime for high temperature applications.

4. CONCLUSION

The structure of EUV reflecting Mo/Si based multilayers has been studied under thermal loading using TEM, hard x-ray diffraction, and XPS. From changes in the multilayer period, detected by grazing incidence x-ray reflectometry, the process of interlayer formation can be investigated in the very early stage of interlayer growth (period changes << 0.1 nm), where classical methods for studying diffusion cannot be applied. $MoSi_2$ formation at the interfaces was found to be the dominant process resulting in optics degradation, with interlayer growth rates independent of the Mo-to-Si ratio, ruling out changes in the bulk of the Mo and Si layers. Diffusion constants obtained from fitting of a parabolic growth law to the experimental data suggests Arrhenius-type behavior in the investigated temperature range from 100 – 275 °C.

The thermal behavior of Mo/Si coatings was compared to that of three multilayer types designed for enhanced thermal stability. A multilayer system designed for high reflectance using Si_3N_4 diffusion barrier layers at the Mo-on-Si interfaces showed reduced thermal damage upon annealing, where the Si_3N_4 layer remains stable upon annealing. For B_4C barrier layers, the diffusion behavior is more complex, suggesting initial formation of carbides and borides, followed by $MoSi_2$ formation. A third multilayer system that is based on replacing the Mo layers with Mo_2C to prevent $MoSi_2$ formation showed thermal stability comparable to the multilayer with B4C interfaces, although at a reduced EUV reflectivity. All multilayer designs exhibited Arrhenius-type behavior with diffusion constants reduced by several orders of magnitude compared to Mo/Si. Effective activation energies can be used to determine the impact of thermal annealing on optical performance at a specified temperature, where caution must be taken when extrapolating to extremely low or high temperatures, where other interface processes may become important in determining thermal damage.

5. ACKNOWLEDGEMENTS

This work is part of the FOM Industrial Partnership Programmes I10 (‘XMO’) and I23 (‘CP3E’) which are carried out under contract with Carl Zeiss SMT GmbH, Oberkochen, ASML, Veldhoven, and the ‘Stichting voor Fundamenteel Onderzoek der Materie (FOM)’, the latter being financially supported by the ‘Nederlandse Organisatie voor Wetenschappelijk Onderzoek (NWO)’. Furthermore, part of the work is carried out in the EXEPT research programme funded by AgentschapNL.

Downloaded From: https://www.spiedigitallibrary.org/conference-proceedings-of-spie on 2/28/2018 Terms of Use: https://www.spiedigitallibrary.org/terms-of-use

REFERENCES

[1] Kirz, J., Jacobsen, C. and Howells, M., "Soft X-ray microscopes and their biological applications", Quarterly Reviews of Biophysics 28(1), 33-130 (1995)

[2] Lindblom, J.F., Walker, A.B.C., Barbee and T.W., Jr., "Normal incidence reflection multilayer optics for solar soft X-ray/extreme ultraviolet (XUV) observations", Proceedings of SPIE meeting on X-ray imaging II, 11-19 (1986)

[3] Chapman, H.N., Hau-Riege, S.P., Bogan, M.J., Bajt, S., Barty, A., Boutet, S., Marchesini, S., Frank M., et al. "Femtosecond time-delay X-ray holography" Nature 448(7154), 676(2007)

[4] Mirkarimi, P.B., "Stress, reflectance, and temporal stability of sputter-deposited Mo Si and Mo Be multilayer films for extreme ultraviolet lithography", Optical Engineering 38(7), 1246-1259 (1999)

[5] Tümmler, J., Scholze, F., Brandt, G., Meyer, B., Scholz, F., Vogel, K., Ulm, V., Poier, M., Klein, U. and Diete, W., "New PTB reflectometer for the characterization of large optics for the extreme ultraviolet spectral region", Proceedings SPIE 4688, 338-347 (2002)

[6] Stearns, D. G., Stearns, M. B., Cheng, Y., Stith, J. H. and Ceglio, N. M., "Thermally induced structural modification of Mo/Si multilayers", Journal of Applied Physics 67(5), 2415-2427 (1990)

[7] Attwood, D., [Soft X-rays and Extreme Ultraviolet Radiation – Principles and Applications], Cambridge University Press, Cambridge (1999).

[8] Windt, D.L., "IMD - software for modeling the optical properties of multilayer films", Computers in Physics 12(4), 360 (1998)

[9] Nedelcu, I., van de Kruijs, R.W.E., Yakshin, A. E. and Bijkerk, F., "Thermally enhanced interdiffusion in Mo/Si multilayers", Journal of Appl. Phys. 103(8), 083549-083549-6 (2008).

[10] Nedelcu, I., van de Kruijs, R.W.E., Yakshin, A. E. and Bijkerk, F., "Temperature dependent nano-crystal formation in Mo/Si multilayers", Physical Review B 76(24), 245404(2007)

[11] Jost, W., [Diffusion in solids, liquids, gases], Academic press inc., New York (1952).

[12] Bruijn, S., van de Kruijs, R.W.E., Yakshin, A.E. and F. Bijkerk, "In-situ study of the diffusion-reaction mechanism in Mo/Si multilayered films," Applied Surface Science 257, 2707-2711 (2011).

[13] Nicolet, M.A., "Diffusion barriers in thin films", Thin Solid Films 52, 415-443 (1978)

[14] de Rooij-Lohmann, V., Veldhuizen, L.W., Zoethout, E., Yakshin, A.E., van de Kruijs, R.W.E., Thijsse, B.J., Gorgoi, M., Schafers, F. and Bijkerk, F., "Chemical interaction of B4C, B, and C with Mo/Si layered structures", Journal of Applied Physics 108(9), 094314 (2010)

[15] Rosen, R.S., Stearns, D.G., Viliardos, M.A., Kassner, M.E., Vernon, S.P., and Cheng, Y., "Silicide layer growth rates in Mo/Si multilayers", Applied Optics 32, 6975 (1993)

[16] Bruijn, S., van de Kruijs, R.W.E., Yakshin, A.E. and F. Bijkerk, "Ion assisted growth of B_4C diffusion barrier layers in Mo/Si multilayered structures", Journal of Applied Physics (submitted), (2011)

Downloaded From: https://www.spiedigitallibrary.org/conference-proceedings-of-spie on 2/28/2018 Terms of Use: https://www.spiedigitallibrary.org/terms-of-use